Development of Wireless In-wheel Motors for Dynamic Charging

– from 2nd to 3rd generation –

Hiroshi Fujimoto
Dept. of Advanced Energy
Graduate School of Frontier Science
The University of Tokyo
Kashiwa, Japan
fujimoto@k.u-tokyo.ac.jp

Osamu Shimizu
Dept. of Advanced Energy
Graduate School of Frontier Science
The University of Tokyo
Kashiwa, Japan
shimizu.osamu@edu.k.u-tokyo.ac.jp

Sakahisa Nagai
Dept. of Advanced Energy
Graduate School of Frontier Science
The University of Tokyo
Kashiwa, Japan
nagai-saka@edu.k.u-tokyo.ac.jp

Toshiyuki Fujita
Dept. of Advanced Energy
Graduate School of Frontier Science
The University of Tokyo
Kashiwa, Japan
t-fujita@edu.k.u-tokyo.ac.jp

Daisuke Gunji
Powertrain Tech. Dev. Dept.
NSK Ltd.
Fujisawa, Japan
gunji-d@nsk.com

Yoichi Ohmori
Engineering Research Dev.
Research Laboratory
Toyo Denki Seizo K.K.
Yokohama, Japan
oomoriy@toyodenki.co.jp

***Abstract*—In this study, a second-generation wireless in-wheel motor (W-IWM2) having the capability of dynamic wireless power transfer (D-WPT) on its wheel side has been developed. The D-WPT technology can drastically extend the driving range of electric vehicles. In addition, a lithium-ion capacitor (LiC) is installed at the wheel side of the W-IWM2. The LiC can effectively charge the regenerative breaking energy. The W-IWM3, which is an evolution of the W-IWM2, is also developed to reduce the size and to increase the power. This paper describes the development of the W-IWM2 and W-IWM3 with the experimental results.**

***Index Terms*—Electric vehicles, wireless power transmission, in-wheel motor, dynamic wireless power transfer**

I. Introduction

Electric vehicles (EVs) are attracting increasing attention in recent years due to their high environmental performance. The drive train of EVs is an on-board motor system or in-wheel motor (IWM) system. In the IWM, the motor is placed inside the wheel, which has advantages such as improved motion control performance and cruising distance though an independent control of each wheel and a lower weight from the reduction of the number of parts in the driving system [1]. However, the IWM has not been commercialized in mass-produced vehicles due to the limitation of durability, given that the power line connecting the motor and the vehicle's body becomes disconnected through continuous bending or through the impact force arising when the vehicle is running.

Accordingly, the authors have developed the first-generation wireless in-wheel motor (W-IWM1), which eliminates the need for wires between the vehicle's body and the wheels by using the wireless power transfer (WPT) technology, to solve this problem [2]. The developed W-IWM1 achieved the maximum output of 3.3 kW per wheel and the transmission efficiency of 94.3% including the power conversion circuit, and successfully operated the actual vehicle [6]. Controlling transmitting energies only using the phase shift was also reported [3].

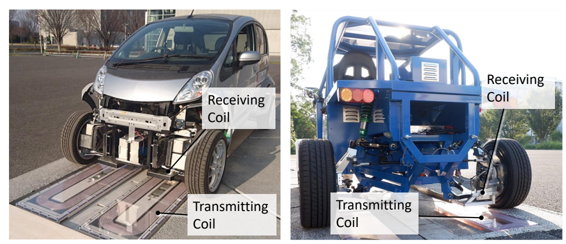

(a) W-IWM2 (b) W-IWM3

Fig. 1. Test vehicles with W-IWM

However, EVs have a shorter cruising distance per charge than conventional internal combustion vehicles. Accordingly, the torque and speed of the motor have been optimized to solve this problem using vehicle speed control [4], [5]. The dynamic WPT (D-WPT) from the equipment installed on the road for vehicles in motion is expected to solve the problem of not only the cruising distance [7] but also the drive efficiency [8]. However, conventional studies of D-WPT assumed that on-board motor type EVs and in-vehicle batteries are charged through the coil installed on the bottom surface of the vehicle. Therefore, we propose a novel method of D-WPT for vehicles in motion, which is suitable for IWMs. That is, instead of transferring electricity from a road coil to a body coil, power is transferred directly to the IWM from the road coil while

Table I
SPECIFICATIONS OF THE TEST VEHICLE FOR W-IWM2

Max. motor power	12 kW
Max. motor torque	76.4 Nm
Reduction ratio	4.407
Number of motors	2 (4)
Total power	24 kW (48 kW)
Total wheel torque	672 Nm (1344 Nm)

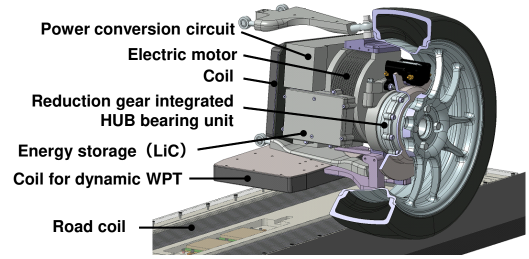

Fig. 2. Configuration of the W-IWM2

the vehicle is moving. To verify this concept on a real vehicle, we developed the second-generation wireless in-wheel motor (W-IWM2) with D-WPT for a vehicle in motion. Moreover, the third-generation wireless in-wheel motor (W-IWM3) is proposed. The W-IWM3 shows improvements in the WPT power, motor output, and size. The W-IWM2 can be employed as a front unit of vehicles, whereas W-IWM3 can be employed as a rear unit.

II. DYNAMIC WIRELESS POWER TRANSFER FOR IWMS

A. Concept of W-IWM2

Several previous studies [9] assumed that a battery of an on-board motor type EV is charged by wirelessly transferring power to the coil installed at the bottom of the car body from the coil installed on the road surface. In [10], a novel D-WPT method was proposed to transfer power to the IWM directly from the coils on the road, as a new-type D-WPT unique to the IWM.

The following are the advantages of the proposed method compared with the conventional dynamic WPT:

1) A high efficiency can be achieved because the power is directly delivered to motors.
2) The power-receiving coil is arranged in the IWM, the air gap with the road surface coil is maintained constant even when the suspension is displaced, and the air gap is minimized.
3) As power is supplied to each wheel, the output per road coil can be reduced.

The specifications of the developed W-IWM2 are listed in Table I. Currently, it is mounted only on the front wheels of the experimental vehicle. However, if it is mounted on all four wheels, the driving performance is equivalent to that of a commercially available EV, which is used as the basis for the experimental vehicle.

B. Configuration of W-IWM2

Fig. 1(a) and Fig. 2 show the experimental vehicle equipped with the developed W-IWM2 on the front wheels and its configuration, respectively. This developed prototype has an IWM with a built-in electromechanical structure, in which a motor, power conversion circuit, control unit, and two wireless power supply coils are arranged in and around the wheel. Each coil is arranged so as not to interfere with the suspension arm, even when the wheel is steered or when the suspension strokes occur. The coil-to-coil gap between the car body and the IWM is 100 mm, and the coil gap between the road surface and the IWM is also 100 mm. The output of the motor is connected to the wheel via an offset-shaft gear reducer built into the hub-bearing unit.

The three functional features of W-IWM2 are as follows:

1) In-motion D-WPT directly from the road to the IWM
2) Energy management control using an energy storage device embedded in a wheel
3) Bidirectional WPT between the car body and the IWM

As 3) has already been realized in the W-IWM1 reported in [2], the first two functions are described in this paper.

The circuit diagram of the W-IWM2 is shown in Fig. 3. The W-IWM2 uses the magnetic resonance coupling system as a WPT technology. For the resonant circuit, the series-series (SS) compensation system, in which the coil and the resonance capacitor are connected in series, is adopted for both the power-transferring side and the power-receiving side. The carrier frequency is 85 kHz, which is the standard for a WPT in the static charging of EVs [11]. There are two wireless power-transferring paths in the W-IWM2, namely, between the vehicle body side and the IWM side and between the road side and the IWM side. The former has the same configuration as the W-IWM1 [2], and bidirectional WPT is possible. The latter is for realizing the in-motion D-WPT, and it includes a coil and a resonance circuit for receiving the power transmitted from a road coil, and an AC/DC converter in the wheel. The AC/DC converter is connected to the DC link of the IWM.

Furthermore, a lithium-ion capacitor (LiC), which is an energy storage device, is installed in the IWM, as a feature of the W-IWM2. The LiC is connected to the DC link of the IWM via the DC/DC converter. Therefore, the DC link of the IWM has four energy sources, that is: 1) the bidirectional energy transfer with the vehicle body, 2) the energy received by the D-WPT from the road coils, 3) the input and output energy with the LiC, and 4) the energy from the driving and regeneration of the motor. It is necessary to control the DC link voltage at a desired level while properly controlling the energy flow [12]. The energy management control will be described in detail later. The circuit parameters (design values) of the

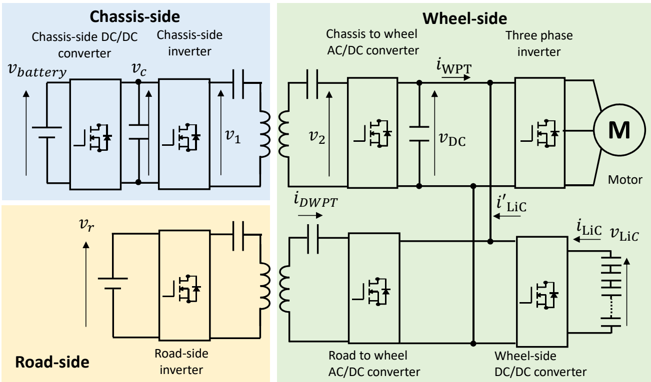

Fig. 3. Circuit configuration of W-IWM2

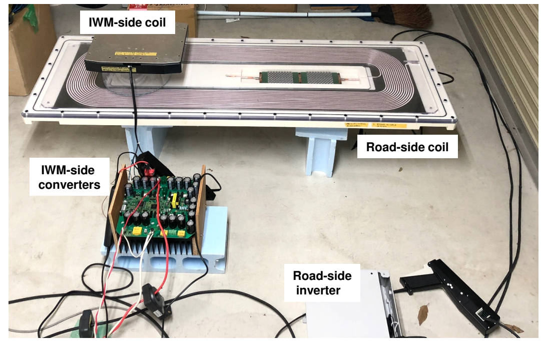

(a) Bench test setup

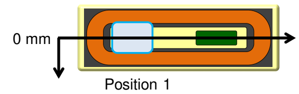

(b) IWM-side coil position1

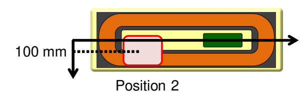

(c) IWM-side coil position2

Fig. 4. Bench test setup of W-IWM2

Table II
TARGET SPECIFICATION OF THE W-IWM2 CIRCUIT (DESIGNED VALUE)

WPT power from Road to IWM	9 kW
WPT power between Chassis and IWM	> 12 kW
Number of LiCs	12 series
Total capacitance of LiCs	125 F
Operation voltage of LiCs	28.8–43.2 V

W-IWM2 are listed in Table II.

III. ROAD-SIDE EQUIPMENT OF D-WPT

This section provides an outline of the road facility of the D-WPT. In previous studies on D-WPT, various circuit configurations were proposed for the road-side equipment [9]. They are roughly divided into the following two groups:

1) Install road coils more than 10 m in length in the direction of travel and drive with large-capacity inverters.
2) Several road coils that are shorter than the vehicle's length are installed and each coil is driven by a small-capacity inverter.

In configuration 1), although only a few inverters are required, there is a need for a large-capacity inverter due to possibility of the presence of multiple EVs in one coil section. In addition, as the wire through which the high-frequency AC flows is longer, there is a higher loss from the wiring and coil.

In contrast, in the configuration 2), the number of inverters increases. However, if the coil length is such that only one EV can be present on each coil, the capacity of each inverter can be small. In addition, by installing each inverter close to the coil, the length of the high-frequency AC wire can be shortened so that the loss from the wiring is low.

IV. EXPERIMENTS OF W-IWM2

In this section, both the measurement results of the efficiency tests at the bench and the results of the D-WPT tests with a real vehicle will be described.

A. Transfer efficiency measurement

1) Experimental methods: As it is difficult to measure the transfer efficiency precisely from the road coil to the IWM via a running test with a real vehicle, it was measured with both coils maintained stationary on the bench. The bench test equipment is shown in Fig. 4 (a). The road coil inverter was connected to a DC power supply, and the transmission power was adjusted by changing the DC voltage value. The operating frequency of the inverter was set to 89 kHz, which is the resonance frequency. A regenerative DC power supply was connected to the DC link of the IWM instead of the motor drive inverter and was operated in the constant-voltage mode, to provide an arbitrary load power to the IWM side circuit. The DC-to-DC transmission efficiency was evaluated by measuring the DC input power on the road side and the DC link power of the IWM with a power meter. Therefore, the measured transmission efficiency includes the efficiencies of the road-side inverter and IWM side converter.

The receiving coil on the IWM side is placed in positions 1 and 2 shown in Fig. 4 (b) and (c). The gap between the coils is approximately 100 mm. In the figure, 1 denotes a position where there is no lateral misalignment and the coupling between the coils is stronger; 2 denotes a position with a lateral misalignment of 100 mm and a weaker coupling.

2) Experimental results of bench test: Table III summarizes the measurement results of efficiency under the condition that the highest powers are obtained at each position. The efficiency of 92.37% was confirmed when the DC input power was 12.532 kW on the road side. Furthermore, a sufficiently high efficiency is realized in the bench tests.

B. D-WPT experiments with real vehicle

The experimental results are shown in Fig. 5, where a moving average filter was applied to remove noise. From Fig. 5 (a) and (b), it can be observed that the vehicle is accelerating owing to the W-IWM2. Fig. 5 (d) presents the current of the

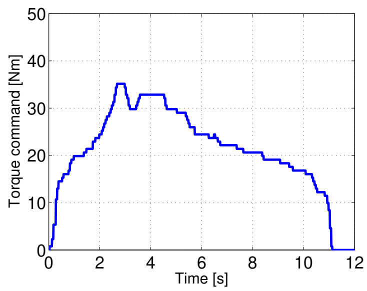

(a) Torque command

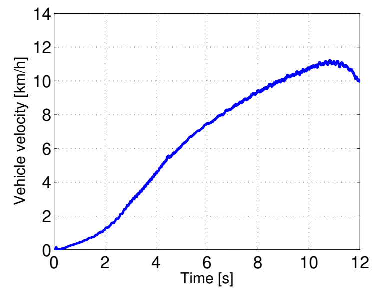

(b) Vehicle velocity

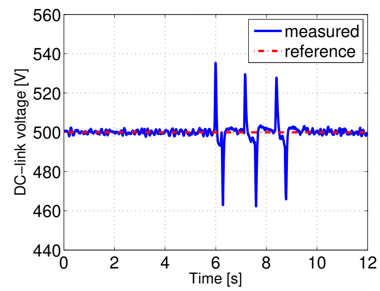

(c) DC-link voltage

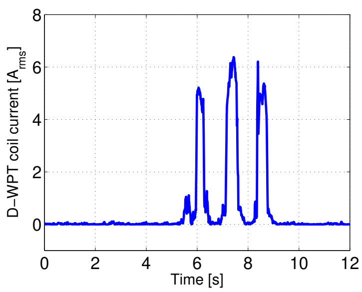

(d) IWM-side D-WPT coil current

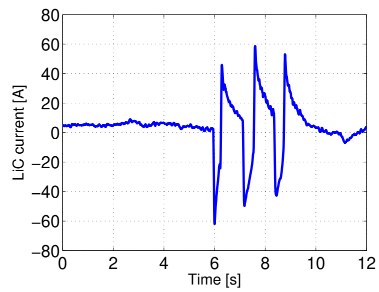

(e) LiC current

Fig. 5. Vehicle test results

Table III
EFFICIENCY MEASUREMENT RESULT OF TEST BENCH (FROM ROAD TO IWM)

IWM-side coil position	Position 1	Position 2
Misalignment	0 mm	100 mm
Operation frequency	89 kHz	89 kHz
Estimated mutual inductance	41.0 μH	25.2 μH
Road-side DC input voltage	578 V	441 V
IWM-side DC-link voltage	575 V	440 V
Road-side DC input	12.532 kW	12.181 kW
IWM-side DC-link input	11.576 kW	10.880 kW
DC-to-DC efficiency	92.37 %	89.32 %

power-receiving coil of the IWM side. It can be confirmed from the time of approximately 5.5 s that the power is being transferred sequentially from the three road coils. Fig. 5 (c) presents the DC link voltage on the IWM side. Although it fluctuates before and after the power transfer when the vehicle is moving, it can be controlled at the target level using the developed control method. As not every current sensor used for the measurement was calibrated, the transmission efficiency was not evaluated.

Fig. 5 (e) presents the current value of the LiC, and the negative current indicates that the LiC is charged. For simplicity, v_{LiC}^{*} is set to be constant in this experiment. The LiC is charged on the road coils and discharged between the road coils.

Based on the above results of the actual vehicle experiments, it was confirmed that the D-WPT in motion was realized in the developed W-IWM2.

Table IV
SPECIFICATION OF THE TEST VEHICLE FOR W-IWM3

Max. motor power	25 kW
Max. motor torque	510 Nm
Reduction ratio	1(Direct Drive)
Number of motors	2 (4)
Total power	50 kW (100 kW)
Total wheel torque	1020 Nm (2040 Nm)

V. DEVELOPMENT OF W-IWM3

A. Concept of W-IWM3

The concept of dynamic charging is the same as that in the W-IWM2. Moreover, all the components for charging and driving of the W-IWM3, i.e., the rectifier, inverter, motor, their control circuit, and liquid cooling system, are inside a wheel. This provides the chassis design more flexibility. The development target of the vehicle category is a mid-sized passenger vehicle. Therefore, the motor output and maximum torque are improved. The adopted wheel size is 17 inch. The specifications of the developed W-IWM3 are listed in Table IV. Currently, it is mounted only on the rear wheels of the experimental vehicle.

B. Configuration of W-IWM3

Fig. 6 shows the experimental vehicle equipped with the developed W-IWM3 on the rear wheels. The three functional features of the W-IWM3 are as follows:

1) In-motion dynamic WPT directly from the road to the IWM

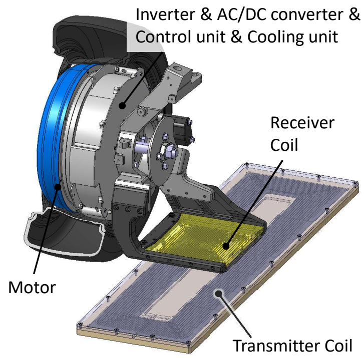

Fig. 6. Structure of the W-IWM3

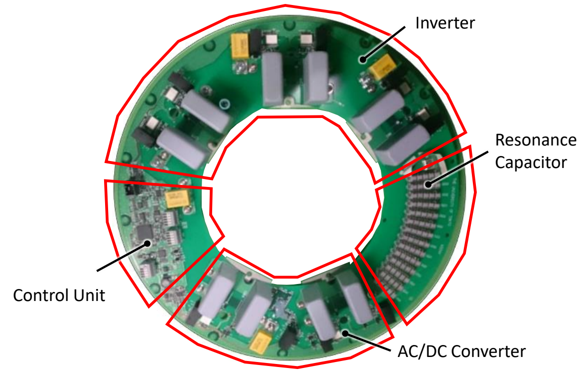

Fig. 7. Circuit board of the W-IWM3

2) Compact layout of the components in a wheel

3) Sufficient motor output and charging input for passenger vehicle

As 1) has already been realized in the W-IWM2, the functions 2) and 3) are described as follows.

The developed prototype has an IWM with a built-in electromechanical structure, in which a motor, power conversion circuit, control unit, and their cooling system are arranged inside the wheel. The coil is arranged so as not to interfere with the suspension arm, even when the wheel is steered or when the suspension strokes occur. The nominal coil-to-coil gap between the road surface and the IWM is 50 mm. The output of the motor is connected directly to the wheel to improve the space factor of the IWM. A direct drive motor has to output high torque by itself. The torque of the motor depends on the width of the motor and the radius of the air-gap. The outer rotor motor can make the radius of the air-gap larger than the inner rotor motor can; therefore, the W-IWM3 adopts the outer rotor.

The circuit board of the inverter and AC/DC converter is designed with a circular shape, to improve the space factor of the IWM. The circuit board of the W-IWM3 is shown in Fig. 7. The inverter, AC/DC converter, resonance capacitor, and their control unit are set on the same circuit board. Thus, the volume of the W-IWM3, which consists of a motor, inverter, AC/DC converter for the receiving coil, and their control unit decreases by 20% compared with that of the W-IWM2. The output power increases by 108% compared with that of the W-IWM2. Therefore, the power density increases by 160%. Current detection control incurs a higher switching loss than voltage detection control due to the phase delay of current sensors in the case of synchronous rectification. To solve this problem, the resonance capacitors are set near the control unit of the AC/DC converter in this system. Thus, the control unit can detect the voltage of the resonance capacitor. This voltage detection method enables the AC/DC converter to control the active rectification with a shorter time-delay than current detection.

The coil design [14] is also improved. Thus, the size, power, and efficiency of the coil of the W-IWM3 are improved simultaneously. The specifications of the coils are listed in Table V. The coil uses a litz wire AWG44x6250 and a set of ferrite cores at the back of the wire. The size of the vehicle-side coil is reduced by 53% and the size of the road-side coil is reduced by 61%. The charging power is increased by 66%, and the loss of the coil is reduced by 45%.

Table V
SPECIFICATION OF THE COILS

W-IWM Generation	W-IWM2	W-IWM3
Vertical of vehicle-side coil	254 mm	230 mm
Horizontal of vehicle-side coil	387 mm	230 mm
Height of vehicle-side coil	37 mm	26.5 mm
Vertical of road-side coil	1500 mm	1086 mm
Horizontal of road-side coil	490 mm	318 mm
Height of road-side coil	45 mm	45 mm
Charging power	12 kW	20 kW
Coil efficiency (measured)	96.5%	98.1%

The circuit diagram of the W-IWM3 is shown in Fig. 8. W-IWM3 also uses the SS circuit for the WPT system. A wireless power-transferring path exists in the W-IWM3 between the road side and the IWM side. This path is used for realizing the D-WPT, and it includes a coil and a resonance circuit for receiving the power transmitted from a road coil, and an AC/DC converter in the wheel. The AC/DC converter is connected to the DC link of the IWM. The battery and DC/DC converter are located on the chassis. The W-IWM3 is developed as the rear unit. Therefore, it is connected to the DC/DC converter by a wire because it does not need to be steered. The WPT system between the chassis and the wheel can be installed to the W-IWM3, when the W-IWM3 is used as a front unit.

VI. Experiments of W-IWM3

In this section, the measurement results of the efficiency tests on the bench will be described. The actual system can control the DC voltage of the transmitter and receiver sides separately. Then, the DC voltage of the receiver side

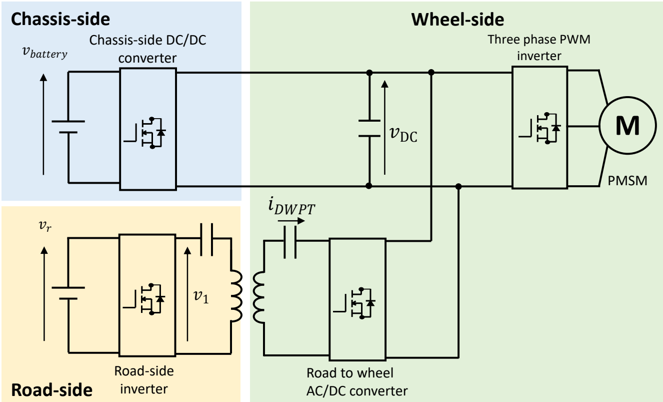

Fig. 8. Circuit configuration of the W-IWM3

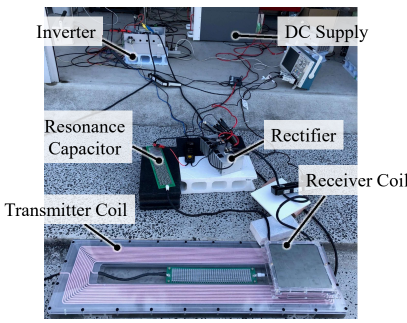

Fig. 9. Test bench of the W-IWM3

is adjusted to achieve the maximum DC-to-DC efficiency. The test bench is shown in Fig. 9. The air gap between the transmitter and receiver coils is 50 mm. The W-IWM3 achieved an output of more than 18 kW with a DC-to-DC efficiency of 95.1%.

VII. Conclusion

In this paper, the second- and third-generation wireless IWMs were introduced. This paper presented a novel D-WPT for a vehicle in motion and its unique application to the IWM. An experimental vehicle equipped with the W-IWM2 on the constructed D-WPT lane was successfully operated by transferring energy from the road coil to the IWM when the vehicle was moving. The D-WPT system in the W-IWM3 could realize sufficient performance for passenger vehicles. In the future, we will consider practical applications such as the generation method of SOC of energy storage and further improve the transmission efficiency by implementing the operating point optimization.

Acknowledgment

This work was partly supported by the JST-Mirai Program (JPMJMI17EM), JSPS KAKENHI (18H03768), and JST-CREST (JPMJCR15K3), Japan.

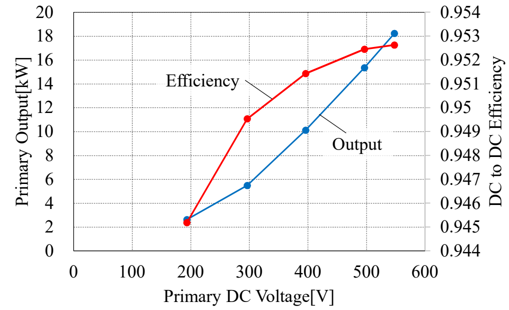

Fig. 10. Experiment result of the W-IWM3

References

[1] S. Murata: "Innovation by in-wheel-motor drive unit, Vehicle System Dynamics", *International journal of Vehicle Mechanics and Mobility*, 50:6, pp. 807–830, 2012

[2] M. Sato, G. Yamamoto, D. Gunji, T. Imura, and H. Fujimoto: "Development of Wireless In-Wheel Motor using Magnetic Resonance Coupling", *IEEE Transactions on Power Electronics*, vol. 31, no. 7, pp. 5270–5278, 2016

[3] G. Lovison, T. Imura, H. Fujimoto, and Y. Hori:"Secondary-side-only Phase-shifting Voltage Stabilization Control with a Single Converter for WPT Systems with Constant Power Load,", *IEEJ J. Industry Applications*, vol. 8, no. 1, pp. 66–74, 2019

[4] H. Fujimoto and S. Harada: "Model-based Range Extension Control System for Electric Vehicles with Front and Rear Driving-Braking Force Distributions", *IEEE Transaction on Industrial Electronics*, vol. 62, no. 5, pp. 3245–3254, 2015

[5] V.-D. Doan, H. Fujimoto, T. Koseki, T. Yasuda, H. Kishi, and T. Fujita:"Iterative Dynamic Programming for Optimal Control Problem with Isoperimetric Constraint and Its Application to Optimal Eco-driving Control of Electric Vehicle," *IEEJ J.Industry Applications*, vol. 7, no. 1, pp. 80–92, 2018

[6] M. Sato, G. Guidi, T. Imura, and H. Fujimoto: "Model for Loss Calculation of Wireless In-Wheel Motor Concept Based on Magnetic Resonant Coupling", *IEEE Workshop on Control and Modeling for Power Electronics*, 2016

[7] G. A. Covic and J. T. Boys: "Modern Trends in Inductive Power Transfer for Transportation Application,", *IEEE Journal of Emerging and Selected Topics in Power Electronics*, vol. 1, no. 1, pp. 28–41, Mar. 2013.

[8] O. Shimizu, S. Nagai, T. Fujita, and H. Fujimoto: "Potential for CO2 Reduction by Dynamic Wireless Power Transfer for Passenger Vehicles in Japan ", *Energies 2020*, vol. 13, pp. 3342, Jun. 2020

[9] C. C. Mi, G. Buja, S. Y. Choi, and C. T. Rim: "Modern Advances in Wireless Power Transfer Systems for Roadway Powered Electric Vehicles", *IEEE Transaction Industrial Electronics.*, vol. 63, no. 10, pp. 6533–6545, 2016

[10] H. Fujimoto, T.Takeuchi, K. Hanajiri, K. Hata, T. Imura, M. Sato, D. Gunji, and G. Guidi: "Development of Second Generation Wireless In-Wheel Motor with Dynamic Wireless Power Transfer", *EVS31 and EVTeC2018*, 2018

[11] SAE International: "J2954 — Wireless Power Transfer for Light-Duty Plug-In/Electric Vehicles and Alignment Methodology," Issued on May 2016, Revised on Nov. 2017.

[12] M. McDonough: "Integration of Inductively Coupled Power Transfer and Hybrid Energy Storage System: A Multiport Power Electronics Interface for Battery-Powered Electric Vehicles," *IEEE Transaction on Power Electronics*, vol. 30, no. 11, pp. 6423–6433, 2015

[13] T. Takeuchi, T. Imura, H. Fujimoto, and Y. Hori: "Power Management of Wireless In-Wheel Motor by SOC Control of Wheel Side Lithium-ion Capacitor", *42nd Annual Conference of the IEEE Industrial Electronics Society*, 2016

[14] Y. Yazaki, W. Ohnishi, T. Imura, H. Fujimoto, K. Sakata, A. Hara, Z. Chen, K. Yokohama, and K. Suzuki: "Development of Multi-axis High-Precision Stage using Multistep Wireless Power Transfer", *45th Annual Conference of the IEEE Industrial Electronics Society*, 2018